Durable antitumor responses to CD47 blockade require adaptive immune stimulation

Jonathan T. Sockolosky[a,b,1], Michael Dougan[c,d,e,1], Jessica R. Ingram[c,d], Chia Chi M. Ho[a,b,f], Monique J. Kauke[g,h], Steven C. Almo[i], Hidde L. Ploegh[c,d,2,3], and K. Christopher Garcia[a,b,j,2,3]

[a]Department of Molecular and Cellular Physiology, Stanford University School of Medicine, Stanford, CA 94305; [b]Department of Structural Biology, Stanford University School of Medicine, Stanford, CA 94305; [c]Department of Biology, Massachusetts Institute of Technology, Cambridge, MA 02142; [d]Whitehead Institute for Biomedical Research, Massachusetts Institute of Technology, Cambridge, MA 02142; [e]Division of Gastroenterology, Department of Medicine, Massachusetts General Hospital, Boston, MA 02114; [f]Department of Bioengineering, Stanford University School of Engineering, Stanford, CA 94305; [g]Department of Chemical Engineering, Massachusetts Institute of Technology, Cambridge, MA 02139; [h]Koch Institute for Integrative Cancer Research, Massachusetts Institute of Technology, Cambridge, MA 02139; [i]Department of Biochemistry, Albert Einstein College of Medicine, Bronx, NY 10461; and [j]Howard Hughes Medical Institute, Stanford University School of Medicine, Stanford, CA 94305

Therapeutic antitumor antibodies treat cancer by mobilizing both innate and adaptive immunity. CD47 is an antiphagocytic ligand exploited by tumor cells to blunt antibody effector functions by transmitting an inhibitory signal through its receptor signal regulatory protein alpha (SIRPα). Interference with the CD47–SIRPα interaction synergizes with tumor-specific monoclonal antibodies to eliminate human tumor xenografts by enhancing macrophage-mediated antibody-dependent cellular phagocytosis (ADCP), but synergy between CD47 blockade and ADCP has yet to be demonstrated in immunocompetent hosts. Here, we show that CD47 blockade alone or in combination with a tumor-specific antibody fails to generate antitumor immunity against syngeneic B16F10 tumors in mice. Durable tumor immunity required programmed death-ligand 1 (PD-L1) blockade in combination with an antitumor antibody, with incorporation of CD47 antagonism substantially improving response rates. Our results highlight an underappreciated contribution of the adaptive immune system to anti-CD47 adjuvant therapy and suggest that targeting both innate and adaptive immune checkpoints can potentiate the vaccinal effect of antitumor antibody therapy.

immunotherapy | protein engineering | cancer | macrophage | T cell

Manipulating the immune system to eliminate tumor cells has recently shown striking clinical efficacy in the treatment of diverse malignancies (1). The therapeutic effect of antitumor antibody treatment generally depends on a combined innate and adaptive antitumor immune response (2–4). Short-acting innate immune effectors, such as natural killer (NK) cells and phagocytes, rapidly kill antibody-opsonized tumor cells via the release of cytotoxins or by physical engulfment, both mediated by antibody engagement of Fc receptors on immune cells. In turn, antibody-dependent tumor cell or antigen phagocytosis (ADCP) by macrophages and dendritic cells (DCs) facilitates immunological memory by presenting processed tumor antigens to T cells with the necessary costimulatory signals to drive clonal T-cell expansion and effector cell differentiation (2). Despite the ability to activate innate and adaptive immunity, antitumor antibody monotherapy is rarely curative; tumor cells have evolved multiple mechanisms to escape immune surveillance, resulting in resistance to antibody therapy and tumor progression.

Up-regulation of CD47 plays an important and seemingly broad role in tumor cell evasion of antibody-dependent clearance by phagocytes. CD47 transmits an inhibitory "don't eat me" signal upon ligation with its receptor signal regulatory protein α (SIRPα), which is expressed primarily on phagocytic cells, including monocytes, macrophages, dendritic cells and neutrophils (5, 6). The antiphagocytic signal delivered by CD47 through SIRPα (7) counterbalances prophagocytic signals delivered by antitumor antibodies upon ligation with activating Fc receptors,

allowing tumor cells to resist macrophage-mediated ADCP (8, 9). Antagonizing the CD47–SIRPα interaction with anti-CD47 antibodies (10) or engineered SIRPα variants (11) synergizes with therapeutic antibodies to promote macrophage-dependent destruction of a broad range of human tumors in mouse xenotransplantation models (9–11). However, whereas innate macrophage responses and their contribution to the efficacy of anti-CD47 therapy are obviously important, the use of immunocompromised hosts in these studies has precluded an assessment of a role for adaptive immunity (10–13).

In vitro, macrophages that phagocytose tumor cells as a result of anti-CD47 antibody treatment can prime antitumor CD8^{+} T-cell responses, suggesting a link between the innate and adaptive immune responses to anti-CD47 therapy (14, 15). Moreover, anti-CD47 antibody therapy promotes an antitumor CD8^{+} T-cell response in syngeneic mouse models of cancer (16), raising the possibility of combining CD47-targeted therapies with T-cell checkpoint blockade to unleash both an innate and adaptive

Significance

Therapeutic antitumor antibodies are widely used clinically. CD47 is an antiphagocytic ligand expressed by tumors that binds the inhibitory receptor signal regulatory protein alpha (SIRPα) on phagocytic cells. Interruption of CD47–SIRPα interactions in immunodeficient mice bearing human tumors enhances therapeutic antitumor antibody responses by promoting phagocytosis of antibody-bound tumor cells. Here, we use a novel anti-CD47 single domain antibody, derived from an alpaca, in an immunocompetent mouse model of melanoma and find that, in contrast to immunodeficient models, CD47 blockade alone is insufficient to enhance the effects of antimelanoma antibodies. However, when combined with blockade of programmed death-ligand 1 (PD-L1), an immune receptor that inhibits antitumor T cell responses, we find synergistic activity, suggesting a role for both innate and adaptive inhibitory pathways in the response to therapeutic antibodies.

antitumor response. Expression of programmed death-ligand 1 (PD-L1) on tumors delivers an inhibitory signal to T cells upon ligation with its receptor PD-1, and antagonizing the PD-1/PD-L1 axis reinvigorates T cells and enhances tumor immunity in both mice and humans (1). Antibody-mediated targeting of PD-L1 on the tumor is particularly attractive because additional immune effector functions independent of PD-1 blockade, such as ADCP, may also contribute to antitumor activity (17).

We sought to investigate the therapeutic potential of combining antitumor antibody therapy with CD47 antagonism and/or T-cell checkpoint blockade. Antibody-based antagonism of CD47 causes mild neutropenia and short term anemia (13, 18) as well as T-cell depletion (19), potentially compromising in vivo efficacy. We generated high-affinity anti-mouse CD47 nanobodies from an immunized alpaca that potently antagonize the CD47–SIRPα interaction but lack effector function due to the absence of an antibody Fc-domain. Using the poorly immunogenic B16F10 syngeneic mouse model of melanoma, we demonstrate that CD47 antagonism synergizes with the B16F10-specific monoclonal antibody TA99 (anti–TRP-1) to promote macrophage-mediated ADCP in vitro; however, this combination therapy was not an effective treatment against B16F10 tumors in vivo. Interestingly, we found that CD47 antagonism synergized with T-cell checkpoint blockade (anti–PD-L1) to promote macrophage phagocytosis of B16F10 cells in vitro and control tumor growth in vivo, which, when further combined with tumor antigen-specific antibody therapy, was curative in a majority of mice. To our knowledge, these experiments are the first demonstration of therapeutic synergy between anti-CD47 and anti–PD-L1 immune checkpoint therapy. Our results support a model whereby the vaccinal effect of tumor antigen-specific antibodies can be enhanced by coantagonism of the CD47/SIRPα and PD-L1/PD-1 immunosuppressive pathways. This combination overcomes innate and adaptive immune resistance to antibody immunotherapy and substantially enhances antitumor responses.

Results

Generation of Mouse CD47-Specific Antagonist Nanobodies. We previously described a strategy to engineer high-affinity SIRPα monomers (CV1) that potently antagonize cell surface CD47 but

do not induce phagocytosis of target cells due to the lack of an Fc domain (11). Instead, CV1 synergized with tumor antigen-specific monoclonal antibodies to potentiate macrophage eradication of human tumor cells while sparing healthy cells. Because CV1 is weakly cross-reactive with mouse SIRPα (11), we lacked an appropriate surrogate for investigating the efficacy of this therapeutic approach, and of combination immunotherapies, in syngeneic cancer models. We therefore sought to isolate alpaca-derived antagonist nanobodies (Nbs) that block mouse CD47 as a tool to probe the biology of the CD47–SIRPα interaction in immune-competent mice. Nbs represent the minimal antigen binding domain (V_HH, ~15 kDa) of heavy chain-only antibodies that naturally occur in camelids. V_HH lack Fc effector functions, are highly stable, are easily produced in large quantities in *Escherichia coli*, and can be readily reformatted as a genetic fusion to alternative protein domains, making them ideal therapeutic and research reagents (20).

To generate mouse CD47 antagonist Nbs, we immunized alpacas with the extracellular Ig-like V-type domain (ECD) of mouse CD47, which is the sole extracellular domain that mediates interaction with SIRPα (6). After one primary immunization and four boosts, peripheral blood lymphocytes (PBLs) were isolated from immunized alpacas, and the extracted RNA was used to construct a V_HH phage display library (Fig. 1A). After two rounds of phage panning against the mouse CD47 ECD, we identified four phage clones that bound mouse CD47 (Fig. S1A). All clones expressed well in *E. coli* and after purification migrate as ~15-kDa monomers by SDS/PAGE (Fig. S1B).

We screened nanobody clones for their ability to antagonize the mouse CD47–SIRPα interaction, using a flow cytometry-based competition assay. We quantified the binding of fluorescent mSIRPα tetramers to the mouse CD47-positive LSTRA tumor cell line (Fig. S2) in the absence or presence of anti-CD47 Nbs. A4, H5, and H9 blocked SIRPα tetramer binding to surface-disposed CD47 whereas F2 had no effect (Fig. S1C). Thus, using an unbiased selection scheme, we identified Nbs that antagonize the mouse CD47–SIRPα interaction.

Anti-CD47 Nanobodies Bind with High Affinity and Specificity to Mouse CD47. To further evaluate the binding properties of the
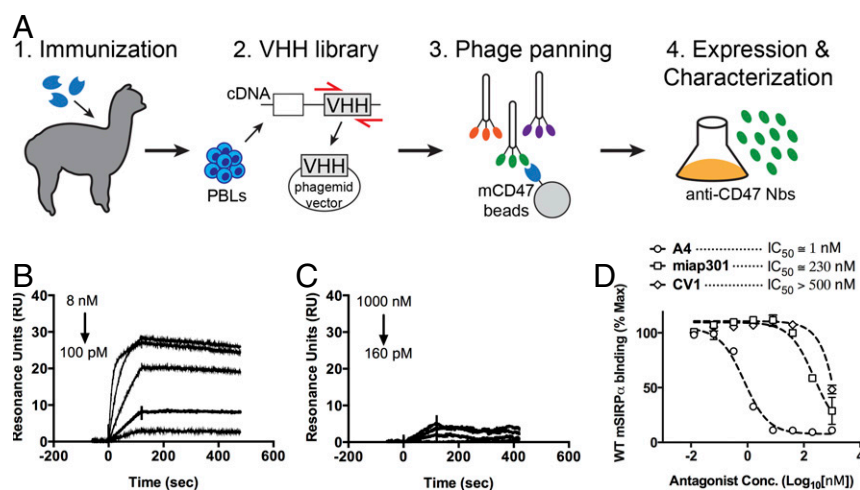

Fig. 1. Characterization of anti-mouse CD47 antagonist nanobody. (*A*) Schematic depicting the generation of anti-mouse CD47 nanobody. An alpaca was immunized with the ECD of mouse CD47, and peripheral blood lymphocytes were isolated and used to create a camelid V_HH phage library for selection of nanobodies that bind the mouse CD47 ECD. (*B* and *C*) Representative surface plasmon resonance (SPR) sensogram of anti-mouse CD47 nanobody A4 binding to immobilized mouse CD47 (*B*) or human CD47 (*C*). All sensograms were baseline-adjusted and reference cell-subtracted. (*D*) Dose–response curves of B16F10 cell surface CD47 antagonism with the anti-mouse CD47 nanobody A4, anti-mouse CD47 antibody miap301, and the anti-human CD47 antagonist CV1. Cells were incubated with increasing concentrations of CD47 antagonists and 100 nM fluorescent SIRPα tetramers for 1 h at 4 °C, washed, and evaluated by FACS. The data shown are the mean (*n* = 3), and error bars indicate SD. Dashed lines represent data fit to a one-site LogIC$_{50}$ model in Prism.

Table 1. Binding affinity and kinetics between anti-mouse CD47 nanobody A4, CV1, and anti-mouse CD47 antibody miap301 immobilized mouse or human CD47

Molecule	Mouse CD47			Human CD47		
	k_a, M^{-1}·s^{-1}	k_d, s^{-1}	K_D, M	k_a, M^{-1}·s^{-1}	k_d, s^{-1}	K_D, M
A4 Nb	2.0×10^7	2.3×10^{-4}	1.2×10^{-11}	—	—	Weak binding
CV1	1.8×10^6	1.1×10^{-2}	6.2×10^{-9}	7.0×10^6	3.7×10^{-5}	5.4×10^{-12}
miap301	1.6×10^5	6.2×10^{-4}	4.0×10^{-9}	n.d.	n.d.	n.d.

n.d., not determined. Dash (—) indicates no significant or quantifiable binding. Sensograms were fit to a 1:1 binding model for derivation of binding kinetics.

anti-CD47 Nbs, as well as their species specificity, we measured binding kinetics by surface plasmon resonance (SPR). A4, H5, and H9 bound immobilized mCD47 with a K_D of ~12 pM, ~50 pM, and ~120 pM, respectively, at pH 7.4 (Table 1, Table S1, Fig. 1B, and Fig. S3). A4 was specific for mouse CD47, with minimal cross-reactivity toward human CD47 at concentrations up to 1 μM (Table 1 and Fig. 1C). In comparison, the human CD47 antagonist CV1 previously generated in our laboratory (11) cross-reacted with mouse CD47, albeit with substantially weaker affinity than A4 (Table 1 and Fig. S3). Although the equilibrium binding affinity of A4, H5, and H9 for mCD47 were similar, the dissociation rate of A4 from mCD47 was approximately three- to fourfold slower than that of H5 or H9 (Table 1), which would be predicted to be beneficial for the antagonist properties of A4 both in vitro and in vivo. Thus, we chose to focus on anti-CD47 Nb clone A4 for further investigation.

A4 Potently Blocks SIRPα Binding to Tumor Cell-Surface CD47. We determined the ability of A4 to antagonize cell-surface CD47 across a range of immortalized mouse CD47$^+$ tumor cell lines (Fig. S2). A4 potently inhibited mSIRPα tetramer binding in a dose-dependent manner to CD47 on all mouse cell lines tested, with an IC$_{50}$ of ~1–5 nM (Fig. 1D and Fig. S4A) but did not antagonize the human CD47–SIRPα interaction (Fig. S4B), in agreement with its species specificity, as determined by SPR. A4 is >200-fold more potent (IC$_{50} \cong$ 1 nM vs. 230 nM) than the commercially available anti-mouse CD47 blocking antibody (miap301) (Fig. 1D). The human CD47 antagonist CV1 is a poor inhibitor of the mouse CD47–SIRPα interaction (IC$_{50}$ > 500 nM) (Fig. 1D) but potently antagonizes the human CD47–SIRPα interaction (IC$_{50} \cong$ 4 nM) (Fig. S4B). Thus, A4 represents a mouse CD47-specific antagonist with binding properties similar to its

human CD47-specific counterpart CV1, with potencies exceeding the commercially available anti-mouse CD47 blocking antibody miap301. Based on these properties, A4 is a suitable CV1 surrogate for investigating the biological consequences of antagonizing CD47 in syngeneic mouse disease models.

Antagonizing Mouse CD47 Potentiates Macrophage-Mediated ADCP of Mouse Tumors Cells. The CD47–SIRPα interaction is a well-known negative regulator of macrophage phagocytosis. We (5, 11) and others (10, 12, 21) have demonstrated that antagonizing tumor cell CD47 binding to SIRPα promotes macrophage effector functions, such as ADCP, which contribute to the eradication of human tumor cells in vitro and human tumor xenografts in vivo. To extend these findings to a syngeneic murine system, we examined the ability of A4 to potentiate antibody-dependent macrophage phagocytosis of tumor cells in vitro, using the mouse melanoma cell line B16F10 as target cells and syngeneic C57BL/6J bone marrow-derived mouse macrophages (BMDMs) as effectors.

Mouse BMDMs were incubated with B16F10 tumor cells opsonized with various combinations of antitumor antibodies and/or anti-CD47 antagonist Nbs. Phagocytosis was quantified by flow cytometry (5, 11). B16F10 cells constitutively expressed the mouse melanoma antigen TRP-1 (gp75) but lacked expression of CD200 (Fig. 2A), which were the targets of the syngeneic mouse IgG2a antibody TA99 and the rat IgG2a antibody OX-90 (22), respectively. Untreated B16F10 cells were poorly phagocytosed by BMDMs, and antagonizing CD47 with A4 alone, or using A4 combined with the negative control antibody OX-90, did not improve macrophage phagocytosis of B16F10 cells (Fig. 2B). Treatment of B16F10 cells with anti–TRP-1 mAb (TA99) induced a significant increase in macrophage phagocytosis; however, the
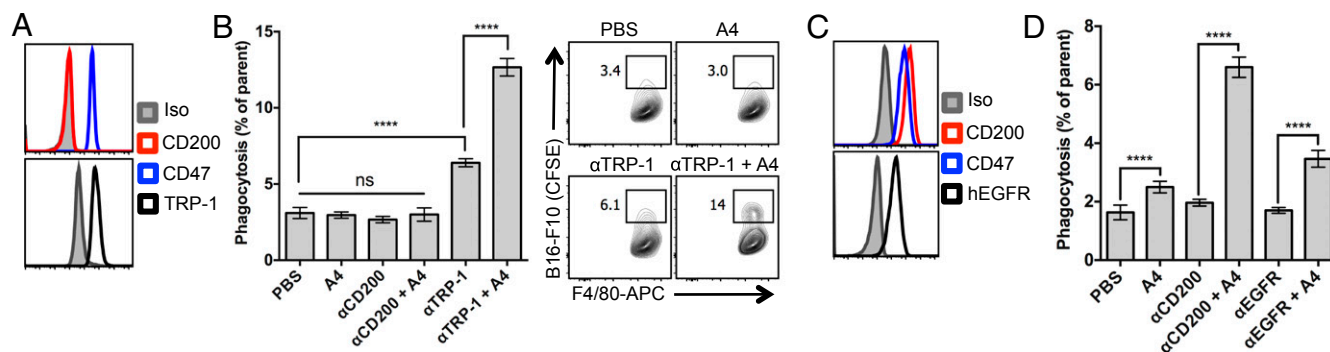

Fig. 2. Anti-mouse CD47 antagonist nanobody enhances macrophage-mediated ADCP. (A) Representative histograms of B16-F10 cell surface CD47, TRP-1, and CD200 expression determined by flow cytometry. (B) Antibody-dependent phagocytosis of B16-F10 cells by bone marrow-derived C57BL/6J mouse macrophages treated with various combinations of control (αCD200) or tumor antigen-specific (αTRP-1) antibody with or without CD47 antagonist nanobody (A4). Phagocytosis is quantified as the percentage of F4/80-positive macrophages that have engulfed CFSE-positive B16-F10 cells as depicted in the representative FACS plots. (C) Representative histograms of Tubo-EGFR cell surface CD200, CD47, and human EGFR (hEGFR) expression determined by flow cytometry. (D) Antibody-dependent phagocytosis of Tubo-EGFR cells by bone marrow-derived BALB/c macrophages as described in B. The data shown are the mean (n = 3), and error bars indicate SD. ****P < 0.0001 determined by one-way analysis of variance test in Prism.

combination of anti–TRP-1 and A4 substantially increased macrophage phagocytosis of B16F10 (Fig. 2B).

To extend these results to an alternative in vitro syngeneic model, we used the BALB/c-derived Tubo-EGFR mouse breast cancer cell line and BALB/c BMDMs as target and effectors, respectively. Tubo-EGFR cells constitutively express mouse CD200 (Fig. 2C) and were previously engineered to express human EGFR (23), which can be targeted by OX-90 (anti-CD200) and the human IgG1 anti-EGFR antibody cetuximab, respectively. Treatment of Tubo-EGFR cells with either anti-CD200 or anti-EGFR mAb alone did not promote ADCP by BMDMs; however, the combination of either anti-CD200 or anti-EGFR with A4 synergized to significantly increase macrophage-mediated ADCP of Tubo-EGFR cells in vitro (Fig. 2D). Consistent with its species-specific binding properties, A4 did not influence human macrophage phagocytosis of human tumor cells whereas the anti-human CD47 antagonist CV1 potentiated ADCP (Fig. S5).

CD47 Antagonism Reveals a Macrophage Effector Function of Anti–PD-L1 Antibodies in Vitro. The efficacy of anti–PD-L1 antibodies in mice is mediated at least in part by Fc receptor (FcR) interactions (17). Although the therapeutic benefit of anti–PD-L1 antibodies in the context of T cells is well-known, to our knowledge,

Fig. 3. IFN-γ exposure inhibits antitumor antibody-dependent macrophage phagocytosis of B16F10 in vitro that can be rescued by combination PD-L1 and CD47 blockade. (A) Representative histograms of B16-F10 cell surface PD-L1, CD47, TRP-1, and CD200 expression before and after overnight treatment with 100 ng/mL IFN-γ as determined by flow cytometry. (B) Antibody-dependent phagocytosis of IFN-γ–treated (gray bars) or untreated (white bars) B16-F10 cells by bone marrow-derived C57BL/6J mouse macrophages treated with various combinations of anti–PD-L1 and/or tumor antigen-specific (αTRP-1) antibody with or without CD47 antagonist nanobody (A4). Phagocytosis is quantified as the percentage of F4/80-positive macrophages that have engulfed CFSE-positive B16-F10 cells as depicted in the representative FACS plots shown in C. The data shown are the mean (n = 3), and error bars indicate SD. ***P < 0.001; ****P < 0.0001 determined by one-way analysis of variance test in Prism.

alternative effector functions of anti–PD-L1 antibodies, such as macrophage ADCP, have not been explored.

We treated B16F10 cells with IFN-γ, denoted B16$^{IFN-γ}$, to induce robust expression of PD-L1 (Fig. 3A), which can be targeted by anti–PD-L1 blocking antibodies. Treatment with anti–PD-L1 mAb (clone 10F.9G2) or A4 alone does not induce macrophage phagocytosis of B16$^{IFN-γ}$ cells compared with a PBS control (Fig. 3B). In contrast, A4 synergizes with anti–PD-L1 to significantly increase macrophage phagocytosis of B16$^{IFN-γ}$ but not untreated B16F10 cells (Fig. 3B). Thus, in addition to activity on T cells, anti–PD-L1 blocking mAbs can also promote macrophage effector functions in vitro that contribute to clearance of PD-L1–expressing tumor cells in the setting of CD47 blockade. The in vivo relevance of this additional mechanism of action of anti–PD-L1 antibodies warrants further investigation because combination immunotherapy with anti–PD-L1 mAbs and CD47 antagonists may synergize to promote a concerted innate and adaptive immune response against tumors. Surprisingly, the anti-mouse CD47 antagonist antibody (miap301) alone or in combination with anti–TRP-1 and/or anti–PD-L1 antibodies failed to potentiate ADCP of B16$^{IFN-γ}$ in vitro (Fig. S6), despite its ability to antagonize the CD47–SIRPα interaction (Fig. 1C). Thus, A4 represents a robust mouse CD47 antagonist that reduces the threshold required to activate macrophage-mediated ADCP by interfering with SIRPα signaling whereas the mechanism of action of miap301 is unclear and may be independent of macrophage phagocytosis.
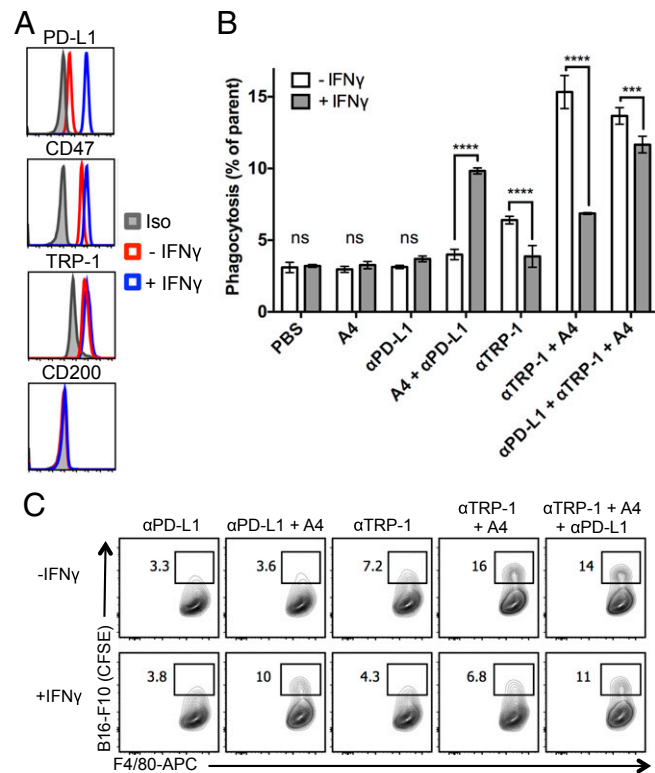
IFN-γ Treatment Impairs Macrophage-Mediated ADCP of B16F10 Cells in Vitro. In the course of our studies with anti–PD-L1, we observed that B16$^{IFN-γ}$ cells were more resistant to anti–TRP-1 mAb-mediated phagocytosis compared with untreated B16F10 (Fig. 3B). To understand whether resistance to anti–TRP-1 mAb-mediated phagocytosis was due to IFN-γ–induced alterations in TRP-1 cell surface levels or other potential negative regulators of macrophage function, we measured B16F10 cell surface levels of TRP-1, CD47, and CD200 (24, 25) by FACS before and after IFN-γ treatment. IFN-γ treatment does not alter B16F10 cell surface TRP-1 or CD200 levels but caused a slight increase in CD47 expression (Fig. 3A), which could account for the reduction in ADCP. However, the defect in anti–TRP-1–mediated phagocytosis of B16$^{IFN-γ}$ cells could not be rescued by antagonizing CD47 with excess A4 (Fig. 3B) (αTRP-1 plus A4), suggesting that increased CD47 expression is not the sole factor that inhibits macrophage-mediated ADCP of B16$^{IFN-γ}$ cells. Addition of anti–PD-L1 partially rescues this phagocytic defect (Fig. 3B) (αPD-L1 plus αTRP-1 plus A4), suggesting that a higher degree of prophagocytic signals is necessary to induce macrophage phagocytosis of B16$^{IFN-γ}$ compared with B10F10 cells. Collectively, these data suggest that IFN-γ may induce expression of alternative, yet unknown negative regulators of macrophage phagocytosis that promote resistance of B16F10 cells to ADCP.

A4 Broadly Recognizes Mouse Hematopoietic and Red Blood Cells but Does Not Cause Erythropenia. Virtually all cells in the body express CD47. Despite broad CD47 expression, toxicities associated with targeting CD47 for therapy in preclinical animal models have been limited to isolated neutropenia and short term anemia (11, 13, 18). We determined the ex vivo reactivity of A4 with various hematopoietic cell populations in the mouse spleen. We also examined potential red blood cell (RBC) and platelet toxicity upon repeated administration of A4. Consistent with the broad expression pattern of CD47, A4 bound all spleen cell populations evaluated, including the following: RBCs, CD19^{+} B cells, CD3^{+} T cells, CD11c^{+} dendritic cells (DCs), CD11c^{+} CD11b^{+} DCs, and CD11b^{+} monocytes, which mirrored the reactivity of the anti-mouse CD47 mAb miap301 (Fig. S7A). Despite reactivity with RBCs, we observed a clinically negligible (~7%) reduction in RBC counts after four consecutive days of

treatment with A4 (Fig. S7B). A mild thrombocytopenia (~30% reduction) was also noted, and all white blood cell counts remained unchanged (Fig. S7C). These alterations in blood counts are in agreement with previous reports indicating that CD47 antagonism alone by CV1 does not substantially alter RBC clearance in the absence of a prophagocytic signal, such as an antibody Fc domain (11).

CD47 Antagonism Does Not Potentiate the Anticancer Activity of the Antitumor mAb TA99 Against Syngeneic B16F10 Tumors. We and others demonstrated that CD47 antagonism synergizes with antitumor antibodies to promote macrophage-mediated tumor eradication across a range of xenogenic mouse models of human cancer (10, 11, 21). However, the nonobese diabetic (NOD)-*scid*, *IL2rg^null* (NSG) mice used in these studies lack an adaptive immune system and have defective innate immunity (26). We sought to extend these findings to syngeneic mouse cancer models to determine whether the efficacy of anti-CD47 adjuvant therapy is preserved in mice with an intact immune system.

B16F10 melanoma cells were injected s.c. onto the back of C57BL/6J mice, and, 4 d post-tumor inoculation, mice were treated systemically with isotype control antibody, TA99 antibody (anti–TRP-1), A4 nanobody (anti-CD47), or the combination of TA99 and A4. A4 monotherapy had no effect on tumor growth or survival whereas TA99 monotherapy slowed tumor growth and modestly improved survival compared with control-treated animals (Fig. 4 A and B). No additional growth or survival benefit was

obtained with combination TA99 and A4 therapy (Fig. 4 A and B) although the data trend toward a slight, albeit nonsignificant, survival advantage. The lack of efficacy of combination therapy in the B16F10 melanoma model contrasts with the efficacy of anti-CD47 combination therapies evaluated in a variety of human solid and blood xenograft tumors (11).

To determine whether this lack of efficacy is the result of an anti-Nb immune response or suboptimal dosing resulting in poor CD47 saturation in vivo, we quantified anti-Nb antibody titers in the serum of A4-treated or control mice by ELISA, as well as the extent of A4 binding to various CD47-positive immune cell types by FACS. A4 treatment did not cause an appreciable antibody response against either an irrelevant control Nb (Nb2) or A4 (Fig. S8A) although one A4-treated mouse evaluated developed low titer (present at <1:100 dilution) antibodies specific for A4. Low titer antibodies reactive against Nb2 and A4 were present in all control Nb2-treated mice (Fig. S8A). These data indicate that A4 treatment is poorly immunogenic, consistent with recent results in humans (27). Analysis of mouse spleen cell populations 24 h after A4 treatment indicates that, at the dose used (200 μg; ~10 mg/kg), ~50% of cell surface CD47 is saturated by A4 (Fig. S8 B and C). Collectively, these data suggest that the lack of efficacy of anti-CD47 adjuvant therapy against B16F10 melanoma is not the result of an anti-A4 immune response or suboptimal A4 dosing. It will be important, moving forward, to determine whether this lack of efficacy is generalizable across various syngeneic mouse
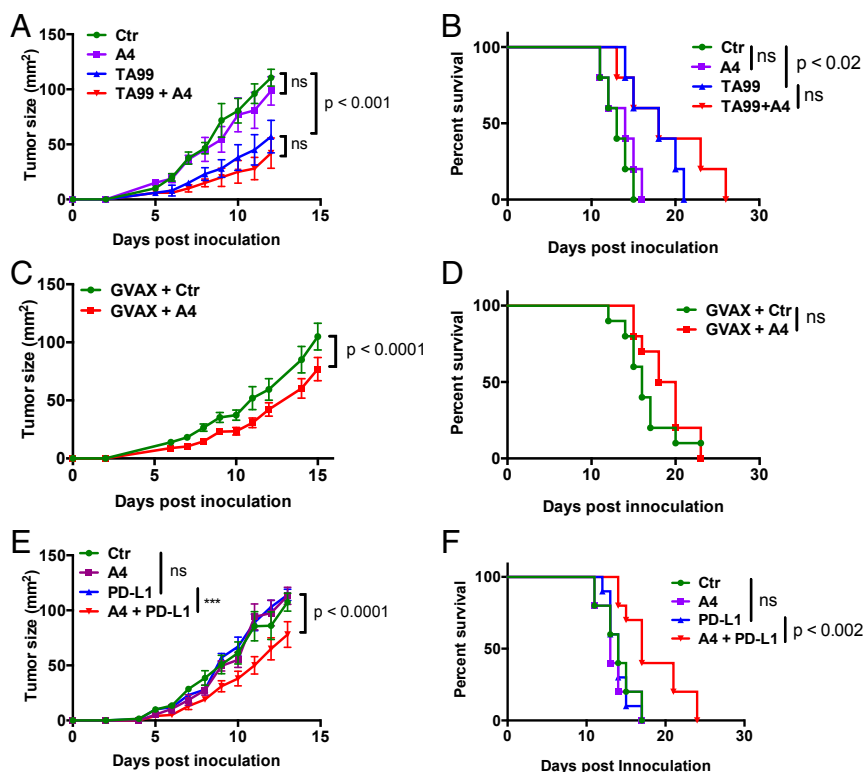

Fig. 4. CD47 antagonism enhances the efficacy of anti–PD-L1 checkpoint blockade therapy but not antitumor antibody or whole-cell vaccination immunotherapy against syngeneic B16-F10 tumors. (A and B) Growth and survival of C57BL/6J mice bearing s.c. B16-F10 tumors treated with control nanobody (Nb), anti-CD47 Nb A4, and/or TA99. Treatment was initiated on day 4 postchallenge. (C and D) Growth and survival of C57BL/6J mice bearing s.c. B16-F10 tumors treated with GVAX and control Nb or GVAX and A4. Treatment was initiated on day 0 postchallenge, and GVAX was administered s.c. on days 0, 4, and 7. Nb was administered daily for 14 d. (E and F) Growth and survival of C57BL/6J mice bearing s.c. B16-F10 tumors treated with control Nb, A4, and/or anti–PD-L1 blocking antibody (10F.9G4). Treatment was initiated on day 0 postchallenge. The data shown in all panels are the mean (n = 10/group) ± SEM and are representative of at least two independent experiments. In all experiments, mice were challenged with 5×10^5 B16F10 cells by s.c. injection and received daily i.p. injections of control Nb or A4 (200 μg), every other day injections of TA99 or anti–PD-L1 (250 μg), or various combinations for 14 d total. Mice were euthanized when tumors reached 125 mm^2, and growth curves are censored after >50% of the mice had been euthanized.

tumors, or specific to the highly tumorigenic, poorly immunogenic B16F10 melanoma model.

CD47 Antagonism Does Not Alter the Antitumor Activity of GM-CSF– Producing B16F10 Tumor Cell Vaccination Therapy. Vaccination represents an alternative strategy to generate endogenous antibodies reactive toward a desired tumor antigen, as well as tumor-specific T-cell responses. To determine whether CD47 blockade can enhance the antitumor activity of whole-cell immunotherapy, mice were inoculated s.c. with B16F10 tumors and immunized with irradiated GM-CSF–producing B16F10 cells (GVAX) on days 0, 4, and 7 postinoculum with or without daily injection of A4 or control compound. GVAX alone was weakly if at all effective at controlling tumor growth and extending survival when given at the time of tumor challenge (Fig. 4D), consistent with previous reports (28, 29). Blockade of CD47 in combination with GVAX resulted in a modest delay in tumor growth, but this delay in tumor growth did not translate to a statistically significant survival advantage (Fig. 4 C and D), despite the presence of B16F10-reactive IgG in the serum of vaccinated mice (Fig. S9). Collectively, these data suggest that CD47 blockade is not sufficient to potentiate the antitumor activity of tumor-specific antibodies, generated through vaccination (Fig. 4 C and D) or passive administration (Fig. 4 A and B), against B16F10 melanomas.

CD47 and PD-L1 Antagonism Synergizes to Control B16F10 Tumor Growth and Extend Survival. Combination immunotherapies that target distinct pathways implicated in cancer immune evasion have shown promise in preclinical mouse cancer models and human clinical trials (30). CD47 and PD-L1 antagonism is believed to elicit therapeutic benefit via distinct mechanisms (phagocytes vs. T cells, respectively). However, we found that anti–PD-L1 antibodies also potentiated macrophage phagocytosis of PD-L1–positive B16F10 cells in vitro when CD47-mediated SIRPα signaling was blocked by A4 (Fig. 3B). Phagocytosed tumor cell antigens presented by macrophages can prime antitumor T-cell responses (14), which may be further bolstered by blocking PD-1/PD-L1 signaling. Therefore, we were interested to determine whether CD47 antagonism synergizes with PD-L1 blockade to promote adaptive immune responses against tumors in vivo.

B16F10 cells were injected s.c. onto the back of C57BL/6J mice and treated with isotype control antibody, anti–PD-L1 antibody (10F.9G2), A4, or the combination of anti–PD-L1 and A4 starting on the day of tumor challenge (day 0). Neither anti–PD-L1 nor A4 administered as monotherapy were effective at controlling tumor growth or extending survival in this model (Fig. 4 E and F). In contrast, combination anti–PD-L1 and A4 therapy resulted in a modest but significant delay in tumor growth, which translated to extended survival (Fig. 4 E and F). Although the combination of anti–PD-L1 and A4 has modest efficacy in the B16F10 melanoma model, we did not observe synergy between anti–PD-L1 and A4 in BALB/c mice bearing syngeneic CT26 tumors (Fig. S10). Interestingly, CT26 was resistant to macrophage-mediated ADCP in vitro (Fig. S11), suggesting a potential explanation for the lack of efficacy in vivo. These data suggest that the efficacy of combination anti-CD47 and anti–PD-L1 therapy is likely dependent on the tumor type and corresponding tumor immunogenicity, as well as the treatment regimen.

Combination CD47 and PD-L1 Blockade Potentiates the Vaccinal Effect of the B16F10-Specific, Anti–TRP-1 Antibody. We observed a modest survival advantage with TA99 monotherapy (Fig. 4 A and B) and combination PD-L1 and A4 therapy (Fig. 4 E and F), as well as a trend toward increased survival when applying the combination of TA99 and A4 (Fig. 4 A and B). Thus, we were interested to determine whether combining PD-L1 and CD47 blockade with the anti–TRP-1 antibody TA99 could stimulate a vaccinal effect against B16F10 by blocking both innate and adaptive immune

checkpoints that limit antibody-dependent immune responses against tumors. Indeed, treatment with the triple combination of TA99, anti–PD-L1, and A4 significantly delayed tumor growth and improved disease-free survival compared with treatment with TA99 and anti–PD-L1 (Fig. 5 A–C). Furthermore, 60% of mice treated with the triple combination remained tumor-free after 42 d, compared with 20% of mice treated with TA99 and anti–PD-L1 (Fig. 5D). Although we did not directly compare single agent or alternative combination treatments in the same experimental group, no alternative treatment regimen evaluated in prior experiments (Fig. 4) cured mice of B16F10 tumors.

To determine whether the combination therapies resulted in durable tumor immunity, surviving mice were rechallenged with B16F10 tumor cells on the contralateral flank 42 d after the initial tumor challenge. Survival was monitored over time. All surviving triple therapy-treated mice were protected against tumor rechallenge (6/6 in TA99 plus anti–PD-L1 plus A4 group), compared with half of the TA99 plus anti–PD-L1 survivors (1/2) and none of the control, previously untreated animals (0/9) (Fig. 5 C and D). Including rechallenge, triple therapy with TA99 plus anti–PD-L1 plus A4 improved overall survival compared with therapy with TA99 plus anti–PD-L1 alone (P = 0.03). One mouse in the triple combination group (TA99, PD-L1, A4) developed mild vitiligo (a reduction of ∼30% of fur pigment), indicative of a T-cell response against shared melanoma and healthy melanocyte antigens (31). Collectively, these data suggest that CD47 antagonism acts to improve the quality and/or magnitude of TA99-induced antitumor immunity, by promoting innate effector functions that drive adaptive immunity. However, resistance to CD47 adjuvant therapy is dominated by adaptive immune suppression, which can be reversed with PD-L1 blockade.

Discussion

Both the innate and adaptive immune system are critical to the efficacy of cytotoxic antibody therapy (3, 4, 23, 32). Expression of CD47 on tumors blunts the therapeutic efficacy of monoclonal antibodies (18, 21). Antibody-mediated blockade of the CD47–SIRPα interaction has shown remarkable preclinical efficacy against a broad range of human tumors in mouse xenotransplantation models (9–11). In immune-compromised hosts (T cell-, NK cell-, and B cell-deficient) bearing tumors, the efficacy of CD47 blockade is macrophage-mediated (10, 13) and depends on the simultaneous inhibition of SIRPα signaling and activation of macrophage FcR (11). However, the use of human xenograft models to study mechanisms governing the efficacy of anti-human CD47 therapeutics has important limitations.

First, these mice lack adaptive immunity and the complex regulatory network of immune cells. These cells create a highly immunosuppressive tumor microenvironment that presents formidable barriers to cancer immunotherapy. Beyond macrophages, CD47 also regulates dendritic cell (DC) and T-cell functions (6, 33–36), emphasizing the importance of studying CD47-targeted therapies in the context of an intact host immune system. Second, the anti-CD47 reagents used in most studies are specific for human CD47; therefore, the only source of targetable CD47 in these human tumor xenograft mouse models is on the tumor itself. By contrast, both humans and mice have a very large antigen sink because virtually all cells in the body express CD47, including red blood cells and platelets, which not only may limit the distribution of anti-CD47 therapies to the tumor but also could mediate toxicity. Third, cross-species differences between the interaction of mouse SIRPα with human CD47, which is ∼10-fold higher than the species-matched affinity, may influence SIRPα signaling and responses to anti-CD47 agents in these models (37), as may differences in other, as yet undefined xenogeneic receptor–ligand interactions. To address these limitations, we generated a potent, anti-mouse CD47-blocking nanobody to probe the wider
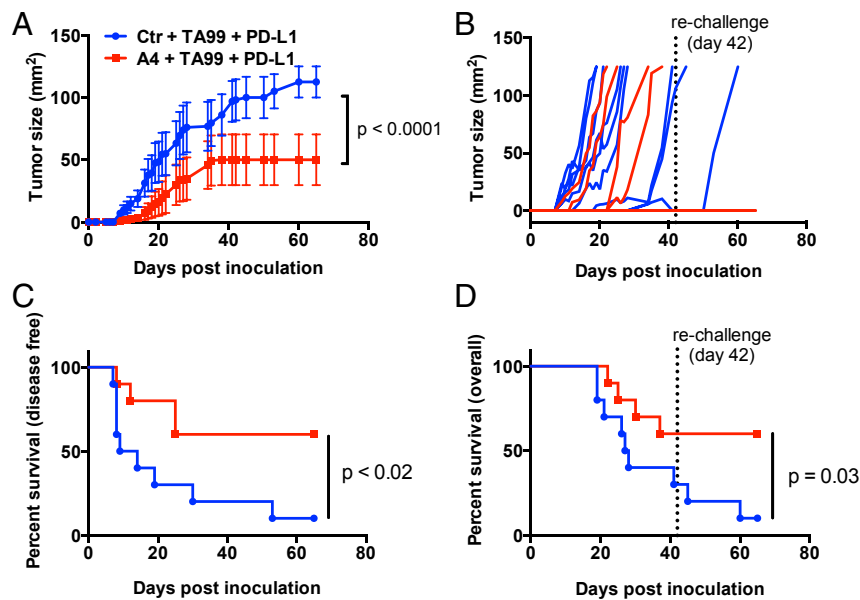
Fig. 5. Combination CD47 and PD-L1 blockade potentiates the vaccinal effect of antitumor antibody immunotherapy against syngeneic B16-F10 tumors. (*A* and *B*) Combined (*A*) and individual (*B*) tumor growth curves, (*C*) disease-free survival, and (*D*) overall survival of C57BL/6J mice bearing s.c. B16F10 tumors treated with control nanobody (Nb) or A4 in combination with TA99 (anti–TRP-1) and anti–PD-L1 (10F.9G4). Mice were challenged with 5×10^5 B16F10 cells by s.c. injection and received daily i.p. injections of control Nb or A4 (200 μg), every other day injections of TA99 or anti–PD-L1 (250 μg), or the various combinations for 14 d total. Treatment was initiated on day 0 postchallenge. Surviving mice from each group ($n = 2/10$ in Ctr plus TA99 plus PD-L1; $n = 6/10$ in A4 plus TA99 plus PD-L1) were rechallenged with 5×10^5 B16F10 tumor cells on day 42 as indicated by the dashed line. The data shown are the combined primary challenge (day 0–42) and secondary challenge (day 42–65). The data shown are the mean ($n = 10$ per group) ± SEM and are representative of two independent experiments. Mice were euthanized when tumors reached 125 mm², and growth curves are censored after >50% of the mice had been euthanized.

immunobiology of CD47 antagonism in a syngeneic system as an adjuvant to antibody immunotherapy in vitro and in vivo.

The best known function of CD47 in the context of cancer immune evasion is inhibition of macrophage phagocytosis (38). Although CD47 may be a dominant antiphagocytic signal presented by all tumor cells (39), we observed that IFN-γ–treated B16F10 cells were more resistant to ADCP in vitro, and this resistance cannot be fully rescued by CD47 blockade (Fig. 3). These observations suggest that additional, unknown tumor cell–effector cell interactions negatively regulate phagocyte function. IFN-γ induces a myriad of changes to the cell surface receptor repertoire on both tumor cells and immune cells (40, 41). In the context of immunotherapy, induction on tumor cells of PD-L1 and MHC class I molecules by IFN-γ is well-known and leads to impaired killing of tumor cells by cytotoxic T cells and NK cells. The identification of alternative IFN-γ–regulated pathways exploited by cancer cells to avoid immune detection, whether dependent or independent of macrophage phagocytosis, will help us understand how cancers evolve and may yield novel therapeutic targets.

Although CD47 antagonism potentiated macrophage-mediated ADCP in vitro, we did not observe therapeutic synergy in vivo by combining an antitumor antibody with the CD47 antagonist nanobody in the B16F10 syngeneic mouse model of melanoma (Fig. 4). The absence of therapeutic synergy with CD47 blockade was true for passive immunization with TA99 mAb, which recognizes a defined tumor antigen (TRP-1, gp75), and for vaccination with GVAX to generate a polyclonal antitumor antibody response. These results raise an important question: Will anti-CD47 monotherapy or combination therapy with antitumor antibodies be as successful in the clinic as in preclinical human tumor xenograft models? Understanding the underlying biology that limits or contributes to the efficacy of CD47 antagonists as cancer immunotherapy adjuvants in immune-competent hosts will therefore be important. The mechanism used may vary

dependent on the tumor type (solid versus hematologic), its immunogenicity, and the corresponding properties of the tumor microenvironment. Extending our findings to alternative syngeneic tumor models, such as hematologic malignancies that are inherently more sensitive to antibody therapy, will therefore be an important next step (3, 10, 23, 32).

Somewhat surprisingly, CD47 blockade improved the in vivo efficacy of the immunomodulatory anti–PD-L1 antibody against B16F10 tumors and, when combined further with TA99, led to durable cures and long-lasting immunity in a majority of mice treated with this triple combination. In contrast, no single agent or dual combination treatment resulted in cures, except for TA99 in combination with anti–PD-L1, which led to durable cures in only 10% of mice. Although speculative, these data suggest that the adjuvant activity of CD47 blockade in combination with tumor antigen-specific (TA99) and T-cell checkpoint antibodies (PD-L1) is mediated by a concerted innate and adaptive immune response, at least in the aggressive B16F10 mouse melanoma model.

We propose a model whereby TA99 binding to TRP-1 on the surface of B16F10 may facilitate FcR-dependent antigen acquisition by tumor-resident DCs or macrophages, either via phagocytosis of apoptotic bodies, whole tumor cells, or trogocytosis (42). CD47 blockade boosts TA99-dependent antigen uptake and presentation by APCs that prime T-cell responses against B16F10, which are enhanced by PD-L1 antagonism. Our model is consistent with mounting evidence that the efficacy of CD47 blockade in immunocompetent hosts depends on the generation of an adaptive antitumor T-cell response (16, 43). Neutrophils also contribute significantly to the efficacy of TA99 mAb therapy in the B16F10 model (4, 44): They are phagocytic and cytotoxic and express SIRPα (5, 21). Thus, CD47 blockade in combination with TA99 may augment antibody-mediated neutrophil responses against tumors. Anti–PD-L1 antibody in combination with CD47 blockade may also mediate depletion of PD-L1+ myeloid-derived suppressor cells (MDSCs). Future mechanistic studies are

warranted to address the relative contribution of various immune cell subsets to the observed efficacy of this combination therapy.

Recently, the efficacy and corresponding mechanism of anti-CD47 antibody monotherapy were evaluated in syngeneic mouse tumor models where DCs, and not macrophages, were held responsible for priming antitumor CD8$^+$ T-cell responses as a result of CD47 blockade (16). The basis for these mechanistic differences between human xenograft (14) and mouse syngeneic cancer models (16) is unclear but may be a result of the anti-CD47 antibody used (miap301) and may be specific to the particular tumor models, and/or other experimental subtleties. DCs are potent stimulators of antitumor T-cell responses, and certain DC subsets express high levels of SIRPα (45); therefore, tumor- or lymphoid-resident DCs could certainly contribute to the efficacy of CD47-targeted therapeutics. The same CD47 blocking antibody (miap301) used by Liu et al. (16) was not effective in an alternative syngeneic mouse breast cancer model, even when administered locally and at high doses (18). Interestingly, we found that miap301 treatment alone or in combination with tumor specific and/or anti–PD-L1 antibodies did not promote macrophage phagocytosis of B16$^{IFN-γ}$ or CT26^{mCD200} cells in vitro (Figs. S6 and S10). Although we have not determined whether miap301 also fails to induce macrophage phagocytosis of the tumor cell models used by Liu et al. (16) and Willingham et al. (18), our results provide a potential explanation for the divergent mechanism reported by Liu et al. (16). Rather than promote macrophage phagocytosis, miap301 may facilitate DC acquisition of miap301-opsonized tumor cell apoptotic bodies. Although our studies do not directly address whether macrophages, dendritic cells, or both contribute to the observed antitumor effect in vivo, our results are highly suggestive of a requirement for professional APCs that phagocytose antibody-opsonized tumor antigens and in turn promote an antitumor T-cell response.

Our results validate the concept of targeting CD47 to overcome innate immune resistance mechanisms that limit the efficacy of antitumor antibody therapy in immune-competent hosts. However, in contrast to previous findings in human xenograft cancer models, where innate macrophage responses to anti-CD47 therapy were sufficient to eradicate tumors (10, 11), durable tumor elimination in the B16F10 syngeneic melanoma model also required PD-L1 blockade. Thus, at least in this model, the reactivation of antibody-dependent innate immunity through CD47 blockade alone is insufficient to overcome adaptive tumor immune resistance to antibody therapy. This may not be true for all cancer models, and some cancers may not require adaptive immune stimulation for anti-CD47 adjuvant therapy to be successful. However, targeting both innate and adaptive immune checkpoints will likely maximize therapeutic effect. Our results support a paradigm whereby resistance to antibody immunotherapy can be overcome by combined innate and adaptive immunomodulation with CD47 and PD-L1 blockade.

Materials and Methods

Cell Culture. B16F10 cells were maintained in Dulbecco's modification of Eagle medium (DMEM) supplemented with 10% (vol/vol) FBS, 1% L-glutamine, and 1% penicillin and streptomycin (P/S). Tubo-EGFR cells were maintained in DMEM supplemented with 10% (vol/vol) FBS, 1% nonessential amino acids (NEAAs), 1% L-glutamine, and 1% P/S. Raji^{GFP}, CT26, and LSTRA cells were maintained in RPMI 1640 supplemented with 10% FBS, 1% L-glutamine, and 1% P/S. All cells were maintained at 37 °C and 5% CO$_2$. B16F10 and CT26 were purchased from ATCC. CT26 cells stably expressing full-length mouse CD200 were generated by lentiviral transduction and selection in 10 μg/mL puromycin. The cDNA encoding full-length mouse CD200 was purchased from Open Biosystems and cloned into pCDH-CMV-MSC-EFI-Puro (System Biosciences). Lentivirus was produced in HEK293 LentiX cells using third generation packaging vectors. CT26^{mCD200} were maintained in RPMI complete supplemented with 10 μg/mL puromycin. LSTRA, Tubo-EGFR,

and Raji^{GFP} cell lines were generously provided by Irving Weissman's laboratory (Stanford University, Stanford, CA).

Affinity Measurements by Surface Plasmon Resonance. SPR measurements were obtained using a BIAcore T100 instrument. The extracellular region of biotinylated mouse or human CD47 was captured on a Biacore SA sensor chip (GE Healthcare) to a final immobilization density of ∼100 resonance units (RUs). A control flow cell with an irrelevant biotinylated protein control captured at the same immobilization density was prepared for reference subtraction. All binding experiments were preformed at 25 °C at a flow rate of 50 μL/min. Serial dilutions of anti-CD47 antibodies, nanobodies, or CV1 in HBS-P$^+$ buffer (GE Healthcare) supplemented with 0.5% (wt/vol) BSA were injected over the SA chip. Binding kinetics were derived by analysis of the generated sensograms fit to a 1:1 binding model using the BIAcore T100 evaluation software.

Cell-Based CD47–SIRPα Competition Assay. Biotinylated WT SIRPα was incubated with Alexa Fluor647-conjugated streptavidin for 15 min at room temperature to form SIRPα tetramers. Adherent cells were harvested by enzymatic dissociation (TrypLE Express; Gibco by Life Technologies), pelleted, washed with autoMACS Running Buffer (PBS, BSA, EDTA, pH 7.2; Miltenyi Biotech), and plated at a density of 50,000 cells per well in a 96-well round-bottom plate. Labeled human (for human cells) or mouse (for mouse cells) SIRPα tetramers at 100 nM (50 μL) were combined with serial dilutions of unlabeled CD47 antagonists (50 μL) in autoMACS Running Buffer and simultaneously added to B16F10, LSTRA, CT26, Tubo-EGFR, or Raji cells for a total volume of 100 μL. Cells were incubated for 1 h at 4 °C, washed with buffer to remove unbound proteins, and analyzed by FACS on a CytoFLEX flow cytometer (Beckman Coulter). Data represent the mean fluorescence intensity normalized to maximal binding for each class of reagents, and points were fit to a one-site LogIC$_{50}$ model using Prism 5 (GraphPad). All data are presented as mean ($n = 3$) ± SD.

In Vitro Mouse Bone Marrow Macrophage-Derived Tumor Cell Phagocytosis Assay. Mouse bone marrow cells were flushed with a syringe from the tibia and femurs of C57BL/6J or BALB/c mice into Iscove's modified Dulbecco's medium (IMDM) supplemented with 10% FBS and 1% P/S. Cells were collected by centrifugation followed by RBC lysis with ammonium–chloride–potassium (ACK) buffer for 3–5 min (Gibco), quenched with complete media, and filtered through a 70-μM cell strainer. Cells were pelleted by centrifugation, resuspended in media containing 10 ng/mL macrophage-colony stimulating factor (M-CSF) (Peprotech), and plated on 4 × 10-cm untreated petri dishes per mouse in 10 mL of media and cultured for 7 d without replenishing or changing media to derive BMDMs.

To quantify antibody-dependent macrophage phagocytosis, tumor cells were harvested by enzymatic dissociation (TrypLE), labeled with carboxyfluorescein succinimidyl ester (CFSE), washed with serum-free IMDM, and plated at a density of 100,000 cells per well in 25 μL serum-free IMDM in a 96-well ultra low attachment round-bottom plate (Cat. no. 7007; Costar) on ice. Tumor cells were opsonized by addition of 25 μL of the various CD47 blocking reagents, antitumor antibodies, or controls for 30 min on ice. BMDMs were harvested by enzymatic dissociation and cell scraping, pelleted, washed in serum-free IMDM, and added to opsonized tumor cells at a density of 50,000 cells per well in 50 μL of media for a final assay volume of 100 μL and an effector-to-tumor cell ratio of 1:2. Cells were incubated at 37 °C for 2 h, pelleted, washed with autoMACS running buffer, and stained with a 1:100 dilution of anti-mouse F4/80-APC (Biolegend) in autoMACS buffer for 1 h at 4 °C. Cells were pelleted, washed, and resuspended in a 1:10,000 dilution of 4′,6-diamidino-2-phenylindole (DAPI) and analyzed by FACS using the CytoFLEX equipped with a high-throughput sampler.

To induce PD-L1 expression for in vitro phagocytosis assays, cells were cultured overnight in mouse IFN-γ (Peprotech) diluted to a final concentration of 100 ng/mL in complete media. Cells were washed thoroughly to remove IFN-γ before harvesting for phagocytosis assay.

Animals. All mice were housed at the Whitehead Institute for Biomedical Research and were maintained according to protocols approved by the Massachusetts Institute of Technology (MIT) Committee on Animal Care. C57BL/6 and BALB/c mice were purchased from The Jackson Laboratory or bred in house. A male alpaca (*Vicugna pacos*) was purchased locally, maintained in pasture, and immunized with a mixture of recombinant mouse and human proteins, including mouse CD47, following a protocol authorized by the Tufts University Cummings Veterinary School Institutional Animal Care and Use Committee (IACUC).

Tumor Models. B16F10 and CT26 cells were purchased from ATCC. B16F10 GM-CSF was a gift from Glenn Dranoff (currently at Novartis Institute for Biomedical Research, Cambridge, MA). For in vivo challenge experiments, 5×10^5 B16F10 cells were inoculated by s.c. injection in 500 μL of Hanks' balanced salt solution (HBSS). For vaccinations, 5×10^5 irradiated (3,500 rad) GM-CSF–secreting B16F10 cells (GVAX) were administered as an s.c. injection in 250 μL of HBSS. V$_H$Hs (200 μg) [anti-CD47 A4 or irrelevant control (96G3m)] were administered daily in 200 μL of LPS Free PBS (TekNova) by i.p. injection for 14 consecutive days. Anti–PD-L1 mAb (250 μg) (10F.9G2; BioXCell) and anti–TRP-1 mAb (TA99; provided by Dane Wittrup, MIT, Cambridge, MA) were administered i.p. every other day in 200 μL of LPS Free PBS for 14 d. Tumor size was measured in two dimensions using precision calipers. Mice were euthanized when the total tumor volume exceeded 125 mm^2. Blood cell counts were obtained by bleeding single agent-treated animals from the tumor treatment studies after 4 d of therapy. Blood samples were analyzed by the Hematology Core Facility at Children's Hospital Boston.

Statistics. Two-sample comparisons used the t test with pooled variance if there was no evidence of inhomogeneity of variances between groups. If the variances were unequal, the exact Wilcoxon rank sum test, a nonparametric alternative to the t test, was used. Every effort was made to keep testing consistent across related experiments. For comparisons of more than two groups, analysis of variance (ANOVA) was used if there was no evidence of inhomogeneity of variance; the Kruskal–Wallis test was the nonparametric alternative. Tumor growth studies were analyzed using mixed model ANOVA.

1. Pardoll DM (2012) The blockade of immune checkpoints in cancer immunotherapy. *Nat Rev Cancer* 12(4):252–264.
2. DiLillo DJ, Ravetch JV (2015) Differential Fc-receptor engagement drives an anti-tumor vaccinal effect. *Cell* 161(5):1035–1045.
3. Park S, et al. (2010) The therapeutic effect of anti-HER2/neu antibody depends on both innate and adaptive immunity. *Cancer Cell* 18(2):160–170.
4. Zhu EF, et al. (2015) Synergistic innate and adaptive immune response to combination immunotherapy with anti-tumor antigen antibodies and extended serum half-life IL-2. *Cancer Cell* 27(4):489–501.
5. Ho CCM, et al. (2015) "Velcro" engineering of high affinity CD47 ectodomain as signal regulatory protein α (SIRPα) antagonists that enhance antibody-dependent cellular phagocytosis. *J Biol Chem* 290(20):12650–12663.
6. Barclay AN, Van den Berg TK (2014) The interaction between signal regulatory protein alpha (SIRPα) and CD47: Structure, function, and therapeutic target. *Annu Rev Immunol* 32:25–50.
7. Tsai RK, Discher DE (2008) Inhibition of "self" engulfment through deactivation of myosin-II at the phagocytic synapse between human cells. *J Cell Biol* 180(5):989–1003.
8. Chao MP, Majeti R, Weissman IL (2011) Programmed cell removal: A new obstacle in the road to developing cancer. *Nat Rev Cancer* 12(1):58–67.
9. Jaiswal S, et al. (2009) CD47 is upregulated on circulating hematopoietic stem cells and leukemia cells to avoid phagocytosis. *Cell* 138(2):271–285.
10. Chao MP, et al. (2010) Anti-CD47 antibody synergizes with rituximab to promote phagocytosis and eradicate non-Hodgkin lymphoma. *Cell* 142(5):699–713.
11. Weiskopf K, et al. (2013) Engineered SIRPα variants as immunotherapeutic adjuvants to anticancer antibodies. *Science* 341(6141):88–91.
12. Theocharides APA, et al. (2012) Disruption of SIRPα signaling in macrophages eliminates human acute myeloid leukemia stem cells in xenografts. *J Exp Med* 209(10):1883–1899.
13. Majeti R, et al. (2009) CD47 is an adverse prognostic factor and therapeutic antibody target on human acute myeloid leukemia stem cells. *Cell* 138(2):286–299.
14. Tseng D, et al. (2013) Anti-CD47 antibody-mediated phagocytosis of cancer by macrophages primes an effective antitumor T-cell response. *Proc Natl Acad Sci USA* 110(27):11103–11108.
15. McCracken MN, Cha AC, Weissman IL (2015) Molecular pathways: Activating T cells after cancer cell phagocytosis from blockade of CD47 "don't eat me" signals. *Clin Cancer Res* 21(16):3597–3601.
16. Liu X, et al. (2015) CD47 blockade triggers T cell-mediated destruction of immunogenic tumors. *Nat Med* 21(10):1209–1215.
17. Dahan R, et al. (2015) FcγRs modulate the anti-tumor activity of antibodies targeting the PD-1/PD-L1 axis. *Cancer Cell* 28(3):285–295.
18. Willingham SB, et al. (2012) The CD47-signal regulatory protein alpha (SIRPa) interaction is a therapeutic target for human solid tumors. *Proc Natl Acad Sci USA* 109(17):6662–6667.
19. Maute RL, et al. (2015) Engineering high-affinity PD-1 variants for optimized immunotherapy and immuno-PET imaging. *Proc Natl Acad Sci USA* 112(47):E6506–E6514.
20. De Meyer T, Muyldermans S, Depicker A (2014) Nanobody-based products as research and diagnostic tools. *Trends Biotechnol* 32(5):263–270.
21. Zhao XW, et al. (2011) CD47-signal regulatory protein-α (SIRPα) interactions form a barrier for antibody-mediated tumor cell destruction. *Proc Natl Acad Sci USA* 108(45):18342–18347.
22. Akkaya M, Aknin M-L, Akkaya B, Barclay AN (2013) Dissection of agonistic and blocking effects of CD200 receptor antibodies. *PLoS One* 8(5):e63325.
23. Yang X, et al. (2013) Cetuximab-mediated tumor regression depends on innate and adaptive immune responses. *Mol Ther* 21(1):91–100.
24. Barclay AN, Brown MH (2006) The SIRP family of receptors and immune regulation. *Nat Rev Immunol* 6(6):457–464.
25. Hoek RM, et al. (2000) Down-regulation of the macrophage lineage through interaction with OX2 (CD200). *Science* 290(5497):1768–1771.
26. Shultz LD, Brehm MA, Garcia-Martinez JV, Greiner DL (2012) Humanized mice for immune system investigation: Progress, promise and challenges. *Nat Rev Immunol* 12(11):786–798.
27. Peyvandi F, et al.; TITAN Investigators (2016) Caplacizumab for acquired thrombotic thrombocytopenic purpura. *N Engl J Med* 374(6):511–522.
28. van Elsas A, Hurwitz AA, Allison JP (1999) Combination immunotherapy of B16 melanoma using anti-cytotoxic T lymphocyte-associated antigen 4 (CTLA-4) and granulocyte/macrophage colony-stimulating factor (GM-CSF)-producing vaccines induces rejection of subcutaneous and metastatic tumors accompanied by autoimmune depigmentation. *J Exp Med* 190(3):355–366.
29. Dougan M, et al. (2010) IAP inhibitors enhance co-stimulation to promote tumor immunity. *J Exp Med* 207(10):2195–2206.
30. Mahoney KM, Rennert PD, Freeman GJ (2015) Combination cancer immunotherapy and new immunomodulatory targets. *Nat Rev Drug Discov* 14(8):561–584.
31. Overwijk WW, et al. (2003) Tumor regression and autoimmunity after reversal of a functionally tolerant state of self-reactive CD8+ T cells. *J Exp Med* 198(4):569–580.
32. Abès R, Gélizé E, Fridman WH, Teillaud J-L (2010) Long-lasting antitumor protection by anti-CD20 antibody through cellular immune response. *Blood* 116(6):926–934.
33. Reinhold MI, Lindberg FP, Kersh GJ, Allen PM, Brown EJ (1997) Costimulation of T cell activation by integrin-associated protein (CD47) is an adhesion-dependent, CD28-independent signaling pathway. *J Exp Med* 185(1):1–11.
34. Yi T, et al. (2015) Splenic dendritic cells survey red blood cells for missing self-CD47 to trigger adaptive immune responses. *Immunity* 43(4):764–775.
35. Seiffert M, et al. (2001) Signal-regulatory protein alpha (SIRPalpha) but not SIRPbeta is involved in T-cell activation, binds to CD47 with high affinity, and is expressed on immature CD34(+)CD38(-) hematopoietic cells. *Blood* 97(9):2741–2749.
36. Ticchioni M, et al. (1997) Integrin-associated protein (CD47) is a comitogenic molecule on CD3-activated human T cells. *J Immunol* 158(2):677–684.
37. Kwong LS, Brown MH, Barclay AN, Hatherley D (2014) Signal-regulatory protein α from the NOD mouse binds human CD47 with an exceptionally high affinity: Implications for engraftment of human cells. *Immunology* 143(1):61–67.
38. Chao MP, Weissman IL, Majeti R (2012) The CD47-SIRPα pathway in cancer immune evasion and potential therapeutic implications. *Curr Opin Immunol* 24(2):225–232.
39. Chao MP, et al. (2010) Calreticulin is the dominant pro-phagocytic signal on multiple human cancers and is counterbalanced by CD47. *Sci Transl Med* 2(63):63ra94.
40. Schroder K, Hertzog PJ, Ravasi T, Hume DA (2004) Interferon-gamma: An overview of signals, mechanisms and functions. *J Leukoc Biol* 75(2):163–189.
41. Furuta J, Inozume T, Harada K, Shimada S (2014) CD271 on melanoma cell is an IFN-γ-inducible immunosuppressive factor that mediates downregulation of melanoma antigens. *J Invest Dermatol* 134(5):1369–1377.
42. Beum PV, Mack DA, Pawluczkowycz AW, Lindorfer MA, Taylor RP (2008) Binding of rituximab, trastuzumab, cetuximab, or mAb T101 to cancer cells promotes trogocytosis mediated by THP-1 cells and monocytes. *J Immunol* 181(11):8120–8132.
43. Soto-Pantoja DR, et al. (2014) CD47 in the tumor microenvironment limits cooperation between antitumor T-cell immunity and radiotherapy. *Cancer Res* 74(23):6771–6783.
44. Albanesi M, et al. (2013) Neutrophils mediate antibody-induced antitumor effects in mice. *Blood* 122(18):3160–3164.
45. Lahoud MH, et al. (2006) Signal regulatory protein molecules are differentially expressed by CD8- dendritic cells. *J Immunol* 177(1):372–382.
46. Maass DR, Sepulveda J, Pernthaner A, Shoemaker CB (2007) Alpaca (Lama pacos) as a convenient source of recombinant camelid heavy chain antibodies (VHHs). *J Immunol Methods* 324(1-2):13–25.